2021 43rd Annual International Conference of the
IEEE Engineering in Medicine & Biology Society (EMBC)
Oct 31 - Nov 4, 2021. Virtual Conference

High Compliance Pneumatic Actuators to Promote Finger Extension in Stroke Survivors

James V. McCall[1], and Derek G. Kamper[1], *Member, IEEE*

Abstract— **Compliant pneumatic systems are well suited for wearable robotic applications. The actuators are lightweight, conformable to irregular shapes, and tolerant of uncontrolled degrees of freedom. These attributes are especially desirable for hand exoskeletons given their space and mass constraints. Creating active digit extension with these exoskeletons is especially critical for clinical populations such as stroke survivors who often have great difficulty opening their paretic hand. To achieve active digit extension with a soft actuator, we have created pneumatic chambers that lie along the palmar surface of the digits. These chambers can directly extend the digits when pressurized. We present a characterization of the extension force and passive flexion resistance generated by these pneumatic chambers across a range of joint angles as a function of cross-sectional shape, dimension, and wall thickness. The chambers were fabricated out of DragonSkin 20 using custom molds and were tested on a custom jig. Extension forces created at the end of the chamber (where fingertip contact would occur) exceeded 3.00 N at relatively low pressure (48.3 kPa). A rectangular cross-section generated higher extension force than a semi-obround cross-sectional shape. Extension force was significantly higher ($p < 0.05$) for actuators with the highest wall thickness compared to those with the thinnest walls. In comparison to previously used polyurethane actuators, the DragonSkin actuators had a much higher extension force for a similar passive bending resistance. Passive bending resistance of the chamber (simulating finger flexion) did not vary significantly with actuator shape, wall thickness, width, or depth. The flexion resistance, however, could be significantly reduced by applying a vacuum. These results provide guidance in designing pneumatic actuators for assisting finger extension and resisting unwanted flexion in the fingers.**

I. INTRODUCTION

For stroke survivors and other clinical populations, voluntary digit extension may be particularly difficult to achieve. Proper digit extension is crucial for opening the hand for object grasp, controlling force direction, and facilitating object release. To assist digit extension, past exoskeleton designs have largely focused on placing rigid actuators on the dorsal side of the hand, with force transmitted to the digits through cables or a rigid mechanical structure. Soft actuators, in contrast, afford the possibility of directly moving the digits. Their ability to conform to irregular shapes gives them an advantage over traditional actuators in terms of fit, comfort and customization for wearable robotics, such as exoskeletons. Soft actuators may be invaluable when actuating the fingers and thumb in the hand, where space is limited, adding mass is costly, and there are many degrees of freedom to control.

Hand exoskeletons using soft actuators have tended to focus on active assistance of flexion rather than extension [1,2]. In past studies, we observed the potential for placing soft pneumatic actuators on the palmar side of the hand. However, this polyurethane-based actuator was difficult to fabricate and customize to different hand sizes and shapes [3–5]. Another group has employed PVC pneumatic actuators, but finger extension torque was limited [6].

The goal of this work was to characterize the performance, in terms of generated fingertip force and passive resistance to bending, of pneumatic finger actuators made from Dragon Skin 20. We assessed these pneumatic chambers with varied characteristics: shape, size, and wall thickness. Each chamber was tested over a range of pressures (0-48.3 kPa) and bending angles (0-75°). Due to the palmar location of the actuator, it is important to balance the trade-off between the ability to create large active extension forces and the need for low passive bending resistance. We hypothesized that extension force would increase with greater bending angle, wall thickness, width and depth and that passive resistance to bending would increase with bending angle, wall thickness, width, and depth. We also expected that chambers with a rectangular cross-section would have higher extension force and passive bending resistance than chambers with a semi-obround shape. Our target extension torque was 0.50 N-m (average extension force deficit of adult stroke survivor with severe hand impairment) [7] and our maximum target passive bending resistance torque was 0.05 N-m to achieve high compliance.

II. METHODS

A. Actuator Design and Fabrication

Pneumatic chambers which would fit along a 7.6 cm long finger were created using molding process. The 3D printed molds were used to cast the elastomer into the desired shapes. The walls were formed between a two-part cavity and an insert placed within the two-part cavity. A platinum-cured silicone rubber, Dragon Skin 20 (Smooth-On, Inc., US), filled the mold to fill the negative space left between the cavity and the insert, thereby forming the actuator. Based on its excellent ability to resist pressure compared to other silicone rubbers [8], Dragon Skin 20 was selected because the material was expected to be sufficiently compliant to produce only a low passive bending resistance while possessing the hardness and tensile strength needed to withstand the required pressures.

Fourteen chambers were created, representing combinations of cross-sectional shape (semi-obround or

[1]J.V. McCall and D.G. Kamper are with the Biomedical Engineering Department, North Carolina State University, Raleigh, NC 27695 USA (jvmccall@ncsu.edu).

978-1-7281-1178-0/21/$31.00 ©2021 IEEE

rectangular) (Fig. 1a), wall thickness (0.8-mm, 1.3-mm, or 1.8-mm), actuator width (7.2 mm, 9.6 mm, 12.1 mm) and depth (7.4 mm, 9.9 mm, 12.4 mm) (Fig. 1b). Changes in wall thickness and actuator width and depth were compared with a baseline dimensions of 1.3-mm, 9.6 mm, and 9.9 mm (Fig. 1b), respectively. Actuator shapes, wall thicknesses, and dimensions were informed by preliminary testing.

Rectangular and semi-obround cross-sections were selected based on preliminary testing and past work [9] that identified the rectangular cross-section as generating the highest extension force and the semi-obround cross-section as having the lowest passive bending resistance out of a wider selection of cross-sectional shapes. Rectangular and semi-obround cross-sections have been successfully used in other pneumatic actuators [10,11]. The semi-obround chambers were fabricated with the same cross-sectional widths and areas as the rectangular chambers (Fig. 1a) to facilitate direct comparison. Additionally, a polyurethane-based air chamber was tested [3] for comparison with the DragonSkin 20.

B. Force Measurement

Actuator extension force and passive bending resistance were measured using a custom fixture which was intended to mimic articulation of a 7.6 cm long finger about the MCP joint (Fig. 2). The tip of the fixture was in contact with a force/torque sensor (Mini40, ATI Industrial Automation, Inc., US) positioned perpendicular to the long axis of the fixture Actuator inflation pressure was computer controlled through a digital-to-analog converter (USB-3101, Measurement Computing, USA) and an electropneumatic servo valve (Proportion Air, USA). Actuators were tested at 5 pressures (0, 6.9, 20.7, 34.5, and 48.3 kPa) within the servo valve's range (0-69.0 kPa) and at 5 bending angles (15°, 30°, 45°, 60°, and 75°). Additionally, a vacuum was applied to each actuator to attempt to reduce passive bending resistance.

C. Data Analysis

Repeated measures ANOVA was performed to determine that effect of the between-sample actuator characteristics (shape, width, depth, and wall thickness) on extension force at the "fingertip". Within-sample factors were joint angle and actuator pressure. Evidence of a significant effect led to post-hoc Tukey tests to examine differences among levels of the significant independent factor. This procedure was repeated for the dependent variable of the fingertip force resulting from passive resistance to bending the actuator.

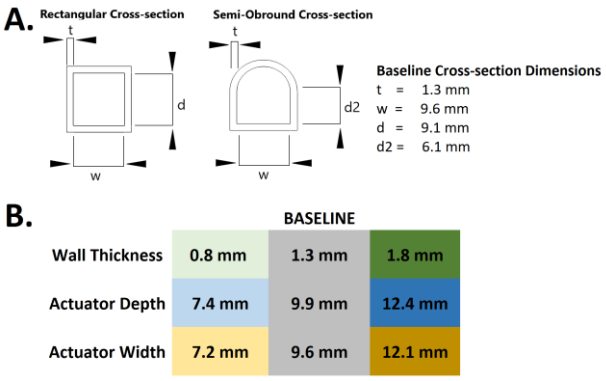

Figure 1. **Actuator Design and Dimensions.** A. Cross-sectional dimensions of the baseline rectangular semi-obround actuators. B. The dimensional variations used to create different actuators.

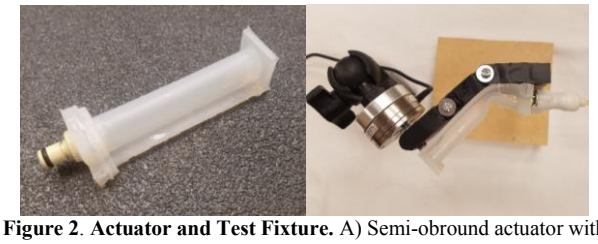

Figure 2. **Actuator and Test Fixture.** A) Semi-obround actuator with overmolded air connector. B) Actuator test setup with loadcell and

III. Results

The fourteen actuators, one for each set of parameters, were successfully fabricated out of DragonSkin 20, After fabrication, uniformity of wall thickness was measured in three chambers with different nominal wall thicknesses. The measured wall thickness for each chamber was (mean±standard deviation): 0.78±0.05 mm, 1.22±0.06 mm, and 1.82±0.04 mm, respectively. On average the mean thickness was within 0.04 mm of the desired value and the standard deviation did not exceed 0.06 mm.

A. Active Extension Force

Actuator characteristics: The 0.8-mm walled actuators were unable to withstand pressures greater than 20.7 kPa, so data was analyzed in two sets. One set (All-Pressures) included all pressures but excluded data from the 0.8-mm actuators, while the other set (All-Thicknesses) included all actuators but excluded pressures greater than 20.7 kPa. For the All-Thicknesses dataset, the between-sample factors of shape ($p=0.01$) and wall thickness ($p = 0.02$) were found to be significant, and each explained a significant portion of the variance in active extension force generated ($\eta p^2=0.71$ and $\eta p^2=0.73$, respectively) (Table I). Extension forces for the rectangular actuators were greater than those for the obround actuators. Post-hoc Tukey test revealed that extension force was greater for the 1.3-mm wall thickness than for the 0.8-mm thickness ($p=0.02$). The extension force did not significantly increase as wall depth and width increased ($p > 0.15$). For the All-Pressures dataset, shape also significantly affected extension force ($p=0.04$), with greater extension forces for the rectangular shape. Depth approached

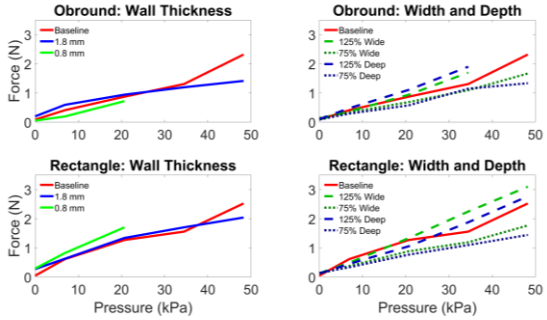

Figure 3. **Extension Force over Range of Pressures.** The extension force created by different actuators for a joint rotation of 45° of flexion across a range of pressures. **Top row**: obround shape. **Bottom row**: rectangular shape. **Left column**: different wall thicknesses. **Right column**: different widths and depths - dotted lines indicate smallest values and dashed lines indicate largest values.

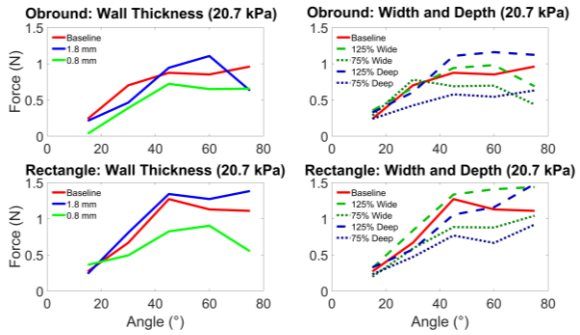

Figure 4. **Extension Force over Range of Flexion Angles.** The extension force created by different actuators pressurized to 20.7 kPa across a range of angles. **Top row**: obround shape. **Bottom row**: rectangular shape. **Left column**: different wall thicknesses. **Right column**: different widths and depths - dotted lines indicate smallest parameter values and dashed lines indicate largest values.

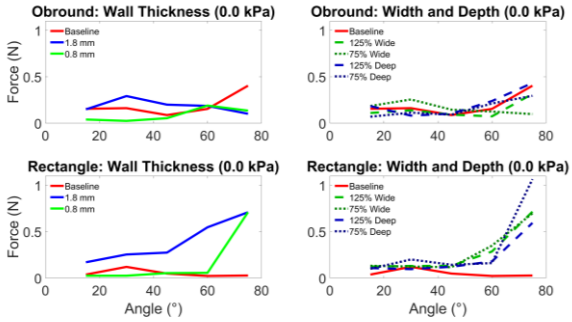

Figure 5. **Passive Bending Resistance over Range of Flexion Angles. Top row**: obround shape. **Bottom row**: rectangular shape. **Left column**: different wall thicknesses. **Right column**: different widths and depths - dotted lines indicate smallest parameter values and dashed lines indicate largest values.

significance (p=0.07); the greatest depth generated 0.50 N more force than the smallest depth.

Actuator pressure: Across actuators, extension force consistently increased as pressure was increased up to 48.3 kPa. (Fig. 3). The within-sample factor of pressure explained a significant amount of the variance for the All Thicknesses and All Pressures datasets (p=0.02, ηp^2=0.66; p=0.04, ηp^2= 0.57, respectively). Maximum fingertip extension forces surpassed 3.00 N for some of the actuators at the 48.3 kPa pressurization. A maximum "fingertip" extension force of 3.57 N was obtained for the rectangular shape with the 1.8-mm wall thickness. This translates into 0.33 N-m of torque at the joint of the test fixture. The relationship of extension force increasing with pressure was typical across all test angles.

Joint angle: Extension force creation tended to be greater at more flexed joint postures across other conditions up to roughly 45° of flexion. Beyond this level of bending, extension force remained fairly constant (Fig. 4). The relationship at 20.7 kPa depicted in Fig. 4 was typical across pressures. The within-sample effect for bending angle was significant and explained a large portion of the variance for the All Thicknesses and All Pressures datasets (p=0.05, ηp^2=0.43; p<0.01, ηp^2=0.84). The two highest extension forces were produced at 75° of flexion (5.35 N for the rectangular shape with the greatest width and 4.84 N for the rectangular cross-sectional shape with the greatest depth. but both actuators underwent plastic deformation at this joint angle and pressure. expanded excessively at this pressure; the deformation during this expansion was plastic but if actuators were placed on adjacent fingers, they would have interfered with each other. The greatest extension force (3.57 N), without excessive expansion, occurred at 60° of flexion.

B. Passive Bending Resistance

Passive bending resistance of the actuators was examined at atmospheric pressure and under a vacuum. At atmospheric pressure, the between-sample effects of actuator shape, thickness, depth, and width were not significant (Table II). Passive bending resistance was 0.07 N higher for the rectangular actuators on average, but the difference was not significant. There was no significant change in force due actuator depth, width, or wall thickness (Fig. 5). The vacuum data are presented as the decrease in passive bending resistance after vacuum was applied. Application of the vacuum flattened the shape of the actuators and decreased passive bending resistance by an average of 0.15±0.08 N. For actuators under vacuum, the thickness, depth, and width had significant between-sample effects (Table II). Passive bending resistance was smaller for the actuators with 1.3-mm thick walls than for those with other wall thicknesses ($p \leq 0.01$), and for actuators with depths of 9.9 mm in comparison to 7.4 mm in depth (p = 0.02). At angles of 15°, and 30°, the vacuum almost eliminated the passive bending resistance. At greater bending angles, it served to limit passive bending resistance to 0.02 N at 45°, 0.13 N at 60°, and 0.38 N at 75°.

IV. Discussion

Wearable, actuated devices for hand rehabilitation are currently being studied for use in a variety of patient populations, including stroke survivors. Many of these individuals need active assistance for digit extension due to limited voluntary activation of digit extensor muscles and involuntary, detrimental activation of digit flexor muscles. Previously developed exoskeletons typically employed rigid actuators such as electric motors to provide extension assistance. These rigid actuators are relatively heavy and bulky. Soft actuators possess potential advantages in terms of

Table I. Repeated Measures Analysis of Extension Force

Between-Sample Effects – All Thicknesses			Average Extension Force - All Thicknesses		
	p	np^2	*Level 1*	*Level 2*	*Level 3*
Shape	0.01	0.71	0.49 *	0.36*	N/A
Thickness	0.02	0.73	0.28*	0.46	0.53*
Depth	0.15	0.47	0.34	0.43	0.49
Width	0.47	0.22	0.39	0.42	0.47

Between-Sample Effects - All Pressures			Average Extension Force - All Pressures		
	p	np^2	*Level 1*	*Level 2*	*Level 3*
Shape	0.04	0.60	0.98*	0.72*	N/A
Thickness	0.69	0.03	0.88	0.81	N/A
Depth	0.07	0.65	0.57	0.91	1.07
Width	0.23	0.44	0 .66	0.91	0.98

Effect Levels 1-3: Shape: Rectangular, semi-obround; Thickness: 0.76mm, 1.27mm, 1.78mm. Depth & Width: 75%, 100%, 125%. * indicates groups are significantly different: p < 0.05.

TABLE II. REPEATED MEASURES ANALYSIS OF PASSIVE BENDING

Between-Sample Effects - Passive Bending			Average Passive Bending Force – Atmospheric pressure (N)		
	p	np^2	*Level 1*	*Level 2*	*Level 3*
Shape	0.27	0.20	0.40	0.33	N/A
Thickness	0.19	0.42	0.36	0.28	0.49
Depth	0.30	0.33	0.44	0.26	0.41
Width	0.35	0.29	0.42	0.27	0.41

Between-Sample Effects - Vacuum			Decrease Passive Bending Force – Vacuum (Δ N)		
	p	np^2	*Level 1*	*Level 2*	*Level 3*
Shape	0.44	0.10	0.07	0.06	N/A
Thickness	0.01	0.86	- 0.02*,†	0.12*	0.10†
Depth	0.02	0.72	0.02*	0.11*	0.07
Width	0.04	0.64	0.03	0.11	0.05

Effect Levels 1-3: Shape: Rectangular, semi-obround; Thickness: 0.76mm, 1.27mm, 1.78mm; Depth & Width: 75, 100, 125%. Symbols indicate significantly different groups: *,† $p < 0.05$

weight, bulk, and flexibility, but have typically been used to create active finger flexion. Palmar actuator placements could provide active digit extension while minimizing joint contact forces. When deflated, the thin chambers permit dexterous manipulation of objects. For the palmar placement, however, a trade-off exists between the potential to provide active extension and the passive resistance to finger flexion created by the presence of the actuators. As clinical populations may exhibit deficits in finger flexion as well as extension, it is important to minimize external flexion resistance.

We designed soft actuators, intended for palmar placement. The actuators were easy to fabricate and required minimal equipment. To minimize passive bending resistance, we did not incorporate features such as torque-compensating layers or complex geometries, such as sinusoidal channels [8] or multiple segments [12]. Actuator shape and wall thickness were found to have the greatest effect on finger extension force, with rectangular actuators having higher extension force and thicker actuator walls increasing extension force at low pressures. Rectangular actuators may have produced higher extension due to their greater surface area resulting in a greater cross-sectional area under pressure, which is associated with greater extension force [13].

The actuators provided substantial extension force at the "fingertip" of the fixture (up to 3.57 N) and extension torque (0.33 N-m) at low pressures. While this is less than the 0.50 N-m target torque, the actuators performed favorably in comparison with other pneumatic actuators, when accounting for differences in actuator size and pressure. Extension torque might be further increased by increasing pressure beyond 48.3 kPa (force increased roughly linearly with pressure). The DragonSkin actuators provided extension forces four times greater than the previous polyurethane actuator [3], and greater torque than PVC actuators at half of the input pressure (0.09 Nm of torque for 96 kPa of pressure)[6]. Actuator extension force increased with bending angle until 45° of bending and remained relatively constant at greater angles. Beyond 45°, kinking in the chamber may have restricted air flow, thereby preventing further force increases. Considerable extension force was still seen, however, even at 75°.

Passive resistance of the chambers to imposed bending was most affected by cross-sectional shape, with rectangular actuators having higher passive bending resistance than semi-obround actuators. Passive bending resistance did not consistently increase as actuator depth, width or wall thickness increased but did tend to increase as the bending angle increased. Applying a vacuum pressure to the actuators significantly decreased the passive bending resistance of the actuators. The vacuum also helped to flatten the pneumatic chambers, thereby providing a low profile. On average, the actuators successfully met the target of less than 0.05 N-m passive bending resistance. The average passive bending torque was 0.02 N-m, and only 0.01 N-m under vacuum.

The actuator with the best balance of extension force and passive bending resistance was the rectangular actuator with 1.3-mm wall thickness and baseline width and depth of 9.6 mm and 9.9 mm. Actuators with baseline depth and width had the lowest passive bending resistance and had similar extension force compared actuators with increased depth or width. However, if a vacuum is used to decrease the passive bending force, then it may be appropriate to focus solely on maximizing extension force. Future work will include cyclic load testing, temperature effects on material performance, and incorporating the actuators into a hand exoskeleton for therapeutic training of manual dexterity.

REFERENCES

[1] Yap HK, Ng HY, Yeow CH. High-Force Soft Printable Pneumatics for Soft Robotic Applications. Soft Robot. 2016;3:144–158.

[2] Tang ZQ, Heung HL, Tong KY, et al. A Probabilistic Model-Based Online Learning Optimal Control Algorithm for Soft Pneumatic Actuators. IEEE Robot. Autom. Lett. 2020;5:1437–1444.

[3] Thielbar KO, Lord TJ, Fischer HC, et al. Training finger individuation with a mechatronic-virtual reality system leads to improved fine motor control post-stroke. J. Neuroeng. Rehabil. 2014;11:1–11.

[4] Lord TJ, Keefe DM. Development of a Haptic Keypad for Training Finger Individuation after Stroke. 2011;1–2.

[5] Simone LK, Sundarrajan N, Luo X, et al. A low cost instrumented glove for extended monitoring and functional hand assessment. J. Neurosci. Methods. 2007;160:335–348.

[6] Nam C, Rong W, Li W, et al. An Exoneuromusculoskeleton for Self-Help Upper Limb Rehabilitation After Stroke. Soft Robot. 2020;00:1–22.

[7] Barry AJ, Kamper DG, Stoykov ME, et al. Characteristics of the severely impaired hand in survivors of stroke with chronic impairments. Top. Stroke Rehabil. 2021;00:1–11.

[8] Yap HK, Lim JH, Nasrallah F, et al. Characterisation and evaluation of soft elastomeric actuators for hand assistive and rehabilitation applications. J. Med. Eng. Technol. 2016;40:199–209.

[9] McCall J V, Readling C, Kamper DG, et al. Compliant Actuators for Hand Exoskeletons. IROS Mech. Des. 2020.

[10] Heung HL, Tang ZQ, Shi XQ, et al. Soft Rehabilitation Actuator With Integrated Post-stroke Finger Spasticity Evaluation. Front. Bioeng. Biotechnol. 2020;8:1–10.

[11] Zhang J, Wang T, Wang J, et al. Geometric Confined Pneumatic Soft–Rigid Hybrid Actuators. Soft Robot. 2020;00:1–9.

[12] Heung KHL, Tong RKY, Lau ATH, et al. Robotic Glove with Soft-Elastic Composite Actuators for Assisting Activities of Daily Living. Soft Robot. 2019;6:289–304.

[13] Shapiro Y, Wolf A, Gabor K. Bi-bellows: Pneumatic bending actuator. Sensors Actuators, A Phys. 2011;167:484–494.